Atomic XAFS as a Tool to Probe the Electronic Properties of Supported Noble Metal Nanoclusters

Ad M. J. van der Eerden,[†] Tom Visser,[†] T. Alexander Nijhuis,[†] Yasuo Ikeda,[‡] Muriel Lepage,[‡] Diek C. Koningsberger,[†] and Bert M. Weckhuysen*,[†]

Department of Inorganic Chemistry and Catalysis, Debye Institute, Utrecht University, Sorbonnelaan 16, 3584 CA Utrecht, The Netherlands, and Material Engineering Division, Toyota Motor Engineering & Manufacturing Europe, Technical Centre, Hoge Wei 33B, B-1930 Zaventem, Belgium

Received November 16, 2004; E-mail: B.M.Weckhuysen@chem.uu.nl

Supported noble metal nanoclusters find widespread applications in heterogeneous catalysis as their catalytic activity can be altered by changing the support composition and architecture or by adding the appropriate promoting elements.[1] These effects are related to changes in the electronic properties of the noble metal, as measured with IR spectroscopy after, for example, CO adsorption. It is generally accepted that the ratio of linear-to-bridged metal-coordinated $C≡O$ reflects the electronic properties of the adsorbing noble metal nanocluster, and this ratio increases with increasing ionization potential of the metal particle.[2]

Another attractive, but almost unexplored, technique for probing the electronic structure of supported noble metal nanoclusters is atomic X-ray absorption fine structure spectroscopy (AXAFS). Holland et al.[3] first recognized this feature, and the groups of Rehr, O'Grady, Baberschke, Ramaker, and Koningsberger did its further development.[4] Whereas extended X-ray absorption fine structure spectroscopy (EXAFS) is known to originate from the scattering of the outgoing electron against the potential of neighboring atoms, AXAFS represents the scattering against the potential of the electron cloud of the absorber atom itself. The embedded potential of probed atoms is dependent on the chemical and electronic environment of the atoms and can be influenced by the support characteristics. The intensity and position of the AXAFS peak is a function of the bonding of the absorbing atom with its environment. Therefore, any change in the support oxide altering the embedded potential of the absorbing noble atom will be reflected in its AXAFS spectrum.

The introduction of AXAFS as a powerful new tool for studying heterogeneous catalysts is hampered by the lack of sufficiently broad experimental data to support the relation between the AXAFS intensity of catalytic systems and the corresponding changes in the electronic properties. Here, we show for a wide set of different support oxides that AXAFS accurately probes the electronic properties of supported Pt nanoclusters. A new tool with the potential to probe the electronic changes in metal catalysts under reaction conditions is explored.

For this purpose, the AXAFS intensities of 14 different supported Pt catalysts [ranging from microporous (H−USY and zeolite Y exchanged with H^+, Na^+, K^+, Rb^+, Mg^{2+}, Ca^{2+}, Sr^{2+}, and Ba^{2+}) over mesoporous (SBA-15 and MCM-41) to macroporous (SiO_2 and SiO_2 loaded with Cs^+ and Ba^{2+}) support oxides] are compared with the corresponding linear-to-bridged Pt-coordinated $C≡O$ ratios as obtained with IR spectroscopy on the same set of samples after adsorption of $C≡O$ at room temperature in the same spectroscopic in situ cell.

---

† Utrecht University.
‡ Toyota Motor Engineering & Manufacturing Europe, Technical Centre.

Supported Pt particles (1 wt %) were prepared via a dry impregnation step of the support oxide materials with the appropriate aqueous solutions of $Pt(NH_3)_4(NO_3)_2$. After impregnation and drying at 353 K in N_2 for 12 h, calcination was carried out by drying in a high air flow for 12 h at 393 K followed by increasing the temperature to 573 K. Reduction was performed in pure H_2 at 573 K for 2 h. After reduction and flushing with N_2 at room temperature, the samples were passivated by admitting a small amount of air. The obtained materials were characterized in detail with XRF, EXAFS, and TEM, and well-defined supported Pt nanoclusters were observed on each of the support oxides (Supporting Information). It was found that the microporous supports contain mainly 1 nm Pt clusters, whereas the main fraction of Pt clusters in the mesoporous and macroporous supports has dimensions around 1.5−2 nm.

The $C≡O$ adsorption IR measurements were performed on self-supported catalyst wafers in a transmission cell. After heating in vacuum and reduction in H_2 at 573 K, the catalyst was exposed to a static pressure of 20 mbar CO, followed by evacuation at room temperature. All IR measurements were duplicated in order to ensure the reproducibility of the obtained results. Figure 1 shows some representative Pt $C≡O$ IR spectra for the samples Pt/K-Y, Pt/Ca-Y, Pt/SiO_2, and Pt/MCM-41. The IR spectra are characterized by a strong IR absorption band at around 2050 cm^{-1} and a weaker, broad band at around 1800 cm^{-1}. The former band is assigned to the stretching vibration of a linearly (L) Pt-coordinated $C≡O$, whereas the latter band is due to bridged (B) $Pt-C≡O$ stretching vibrations.[5] It is clear that the IR L:B intensity ratio obtained by integrating the spectra decreases in the order of Pt/MCM-41 (14) > Pt/SiO_2 (10) > Pt/Ca-Y (4.5) > Pt/K-Y (2.7), reflecting an increasing electron density on the supported Pt nanoclusters. The assumption made is that the extinction coefficients for adsorbed $C≡O$ are influenced to the same extent for the linearly and bridged Pt-coordinated $C≡O$ stretching vibrations, and the error in the ratio is estimated to be around 10%.

Pt L_3 edge XAFS data were collected on self-supported catalyst wafers in a transmission cell, identical to that used for the IR measurements with the exception that the CaF_2 windows have been replaced by Be windows. After measurement, a precise background subtraction was performed, one which optimizes the AXAFS and EXAFS contributions in the XAFS data, while leaving the double-electron excitations mostly in the background (Supporting Information). Details on this procedure can be found elsewhere.[6] The AXAFS contribution is then isolated from the total XAFS data by subtracting the EXAFS contributions from the experimental XAFS data. The error for the isolation of the AXAFS contribution is estimated to be around 10%.[7] The AXAFS spectra of Pt/K-Y, Pt/
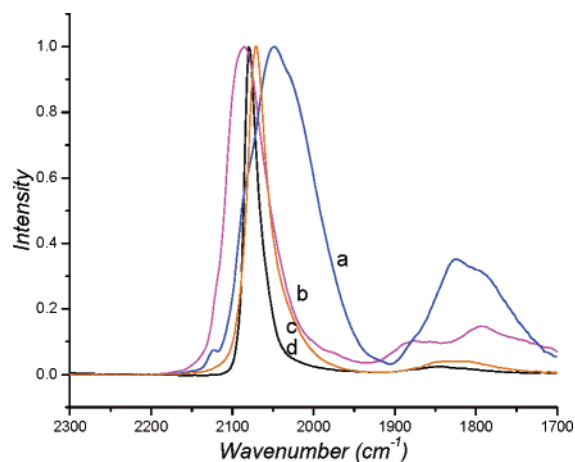
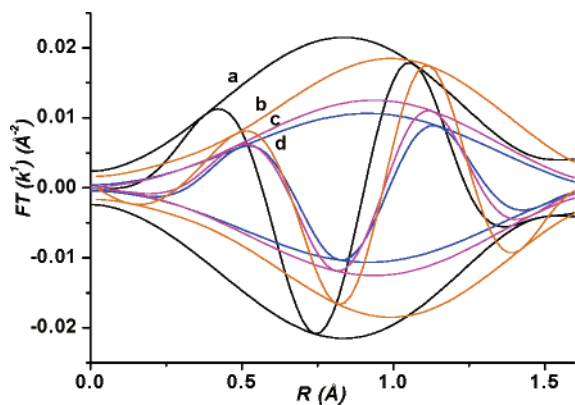**Figure 1.** IR spectra of C≡O adsorbed on (a) Pt/K-Y, (b) Pt/Ca-Y, (c) Pt/SiO₂, and (d) Pt/MCM-41.

Figure 2. Fourier transforms (k^1, $\Delta k = 2.5-8$ Å^{-1}) of the AXAFS spectra of (a) Pt/MCM-41, (b) Pt/SiO₂, (c) Pt/Ca-Y, and (d) Pt/K-Y.

Mg-Y, Pt/SiO₂, and Pt/MCM-41 in the R-range from 0 to 1.5 Å are given in Figure 2. One can notice that the AXAFS data of the different supported Pt nanoclusters differ in their AXAFS intensity, as well in the peak centroid. A decrease in the AXAFS intensity results in a shift of the peak centroid to higher R values, and the AXAFS intensity decrease follows the same order as that of the IR L:B intensity ratios, that is, Pt/MCM-41 (2.2×10^{-2} Å^{-2}) > Pt/SiO₂ (1.6×10^{-2} Å^{-2}) > Pt/Ca-Y (1.25×10^{-2} Å^{-2}) > Pt/K-Y (0.95×10^{-2} Å^{-2}).

The above-described procedure has been applied to the 14 different supported Pt catalysts under study. Figure 3 plots the AXAFS peak intensities of the different samples versus their corresponding IR L:B ratios. The IR L:B ratios span a range of more than 12 units, whereas the AXAFS intensities change between 0.8×10^{-2} and 2.6×10^{-2} Å^{-2}. It is clear that the AXAFS intensity decreases with decreasing IR L:B ratio, and both the AXAFS peak intensity and the IR L:B ratio can be considered as complementary measures for the electron charge of the Pt nanoclusters. In other words, the AXAFS peak intensity and the IR L:B decrease with decreasing ionization potential of the Pt atoms in the nanoclusters.

In conclusion, AXAFS is a very attractive technique for probing the electronic properties of supported noble metal nanoclusters and,
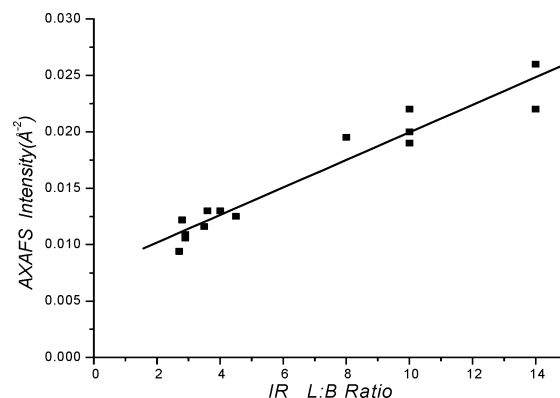

Figure 3. AXAFS peak intensity of supported Pt nanoclusters as a function of the corresponding IR L:B intensity ratio (for error discussion, see text).

in principle, of clusters of any atom amenable to the XAFS technique. In addition, the obtained information is fully consistent with CO IR measurements. More importantly, however, is that AXAFS does not need any probe molecule. As a consequence, AXAFS can be used in the future to probe the electronic properties of supported noble metal nanoparticles under reaction conditions in real time, delivering mechanistic insight on the working catalyst.

Supporting Information Available: Experimental details, an EXAFS analysis sample, and full analysis results (PDF). This material is available free of charge via the Internet at http://pubs.acs.org.

References

(1) (a) Linic, S.; Barteau, M. A. *J. Am. Chem. Soc.* **2004**, *126*, 8086−8087. (b) Bell, A. T. *Science* **2003**, *299*, 1688−1691. (c) Wei, J. M.; Iglesia, E. *Angew. Chem., Int. Ed.* **2004**, *43*, 3685−3688. (d) Carrettin, S.; Concepcion, P.; Corma, A.; Nieto, J. M. L.; Puntes, V. F. *Angew. Chem., Int. Ed.* **2004**, *43*, 2538−2540. (e) Chen, M. S.; Goodman, D. W. *Science* **2004**, *306*, 252−255. (f) Guzman, J.; Gates, B. C. *J. Am. Chem. Soc.* **2004**, *126*, 2672−2673. (g) Derrouiche, S.; Grevejat, P.; Bianchi, D. *J. Am. Chem. Soc.* **2004**, *126*, 13010−13015.

(2) (a) Mojet, B. L.; Miller, J. T.; Koningsberger, D. C. *J. Phys. Chem. B* **1999**, *103*, 2724−2734. (b) van Santen, R. A. *J. Chem. Soc., Faraday Trans. 1* **1987**, *83*, 1915−1934. (c) Crowell, J. E.; Garfunkel, E. L.; Somorjai, G. A. *Surf. Sci.* **1982**, *121*, 303−320. (d) Sheu, L. L.; Karpinski, Z.; Sachtler, W. M. H. *J. Phys. Chem.* **1989**, *93*, 4890−4894.

(3) Holland, B. W.; Pendry, J. B.; Pettifer, R. F.; Bordas, J. *J. Phys. C* **1978**, *11*, 633−642.

(4) (a) Rehr, J. J.; Booth, C. H.; Bridges, F.; Zabinsky, S. I. *Phys. Rev. B* **1994**, *49*, 12347−12350. (b) Wende, H.; Baberschke, K. *J. Electron. Spectrosc. Relat. Phenom.* **1999**, *101−103*, 821−826. (c) Ramaker, D. E.; Mojet, B. L.; O'Grady, W. E.; Koningsberger, D. C. *J. Phys Condens. Mater.* **1998**, *10*, 8753−8770.

(5) (a) Hippe, C.; Lamber, R.; Schulz-Ekloff, G.; Schubert, U. *Catal. Lett.* **1997**, *43*, 195−199. (b) Sheppard, N.; Nguyen, T. T. *Adv. Infrared Raman Spectrosc.* **1978**, *5*, 67−148. (c) Bourane, A.; Dulaurent, O.; Bianchi, D. *J. Catal.* **2000**, *196*, 115−125.

(6) (a) Ramaker, D. E.; van Dorssen, G. E.; Mojet, B. L.; Koningsberger, D. C. *Top. Catal.* **2000**, *10*, 157−165. (b) Koningsberger, D. C.; de Graaf, J.; Mojet, B. L.; Ramaker, D. E.; Miller, J. T. *Appl. Catal. A: General* **2000**, *191*, 205−220.

(7) Tromp, M.; van Bokhoven, J. A.; Slagt, M. Q.; Klein Gebbink, J. M.; van Koten, G.; Ramaker, D. E.; Koningsberger, D. C. *J. Am. Chem. Soc.* **2004**, *126*, 4090−4091.

JA043107L